Transparent Fabry Perot polymer film ultrasound array for backward-mode photoacoustic imaging

Beard PC[1], Zhang EZ, Cox BT

Department of Medical Physics and Bioengineering, University College London, Shropshire House, 11-20 Capper Street, London WC1E 6JA, UK

ABSTRACT

A novel optical ultrasound sensor has been developed for backward-mode photoacoustic imaging. The sensor is based on a Fabry Perot polymer film interferometer, the mirrors of which are transparent to 1064nm, but highly reflective at 850nm. When illuminated by a CW interrogating laser source at the latter wavelength, the system acts as a resonant Fabry Perot (FP) sensing cavity, the reflected intensity output of which is dependent upon acoustically-induced changes in the optical thickness of the polymer film. By optically addressing different regions of the sensor, a notional ultrasound array of arbitrary aperture and dimensionality can be synthesised. The system was demonstrated in backward mode by transmitting 1064nm excitation laser pulses through the sensor into an Intralipid scattering solution (μ_a =0.03mm^{-1}, μ_s'=1mm^{-1}) containing various absorbing structures and detecting the resulting photoacoustic signals over a line. A 1D depth profile of a 1.3mm thick absorbing polymer sheet (μ_a=0.8mm^{-1}) immersed to a depth of 12mm in the Intralipid solution was obtained by performing an 11mm linescan. In another experiment, a 3-layer structure consisting of 0.076mm thick line absorbers was immersed in Intralipid and a 2D image reconstructed from the detected photoacoustic signals using an inverse **k**-space reconstruction algorithm. Lateral resolution was 0.4mm and the vertical resolution 0.1mm. The ability of this system to map wideband photoacoustic signals with high sensitivity in backward mode may provide a useful tool for high resolution imaging of superficial tissue structures such as the skin microvasculature.

1. INTRODUCTION

Photoacoustic imaging is a soft tissue imaging modality which relies upon illuminating a volume of tissue with pulsed visible or NIR laser light. Broadband pulses of acoustic energy are then emitted from preferentially optically absorbing subsurface anatomical structures such as blood vessels and propagate to the surface where they are detected using an array of ultrasound receivers. By measuring the time of arrival of the acoustic pulses at each element of the array, and with knowledge of the speed of sound in tissue, the acoustic signals can be spatially resolved and backprojected, as in conventional medical ultrasound imaging, to form an image of the internally distributed photoacoustic sources. By encoding the spatial distribution of tissue optical properties on to broadband ultrasound waves in this way, the technique combines the advantages of the strong contrast and spectroscopic capability offered by optical methods with the high spatial resolution available to ultrasound. As with many other biomedical optical diagnostic methods, haemoglobin is the most important source of naturally occurring contrast for photoacoustic imaging. Its strong preferential optical absorption at visible and NIR wavelengths and spectroscopic dependence on oxygenation status makes the technique particularly well suited to visualising the structure and function of the vasculature. Applications that exploit this include the assessment of haemodynamic changes in the rat brain[1], the detection of breast tumours[2] and imaging the skin microvasculature[3] for the assessment of dermal vascular lesions[4].

[1] Correspondence to P. Beard, Dept of Medical Physics, UCL, Shropshire House, 11-20 Capper Street, London WC1E 6JA, UK, email: pbeard@medphys.ucl.ac.uk, http://www.medphys.ucl.ac.uk/research/borl/research.htm

Proc. SPIE 5320, pp 230-237, 2004 SPIE BIOS 2004, 25-26 January 2004, San Jose, USA

For short range high resolution applications, such as imaging the skin where it is required to visualise microvessels that lie within a few mm of the surface, it is highly desirable to be able to detect the photoacoustic signals over the same region of the tissue surface that is irradiated: the so-called backward mode of operation. This presents obvious difficulties if an array of piezoelectric detectors is employed. To avoid the detectors obscuring the incident laser beam it is necessary to use a sparsely filled detector array and deliver the laser energy in the space between the elements[5]. However, this inevitably leads to a coarser lateral sampling of the incident acoustic field thus reducing the fidelity of the reconstructed image. The discretisation of the illuminated region may also result in a strongly varying light distribution close to the tissue surface (before the light has reached a depth at which it has lost its directionality and become spatially homogenised), making it more difficult to interpret superficially lying features on the reconstructed image. An alternative approach is to vertically offset the detector from the tissue surface with an optically transparent acoustic coupling medium and illuminate the tissue surface directly beneath the detector with an obliquely incident excitation beam[6] However, this has the disadvantage that the acoustic pathlength is increased with a consequent reduction in both SNR and the effective aperture over which the photoacoustic signals are received.

Optical methods may provide a means of implementing the backward mode of operation. A non-contact interferometric method[7] that employs a probe beam to detect acoustically-induced surface displacements could, in principle, be used in backward mode. A method that has been successfully demonstrated for backward mode imaging is a transparent contact optical ultrasound transducer based upon the detection of acoustically-induced changes in optical reflectance at a glass-liquid interface[8]. In this paper we describe an alternative optical approach based upon the detection of acoustically-induced changes in the optical thickness of a Fabry Perot polymer film interferometer (FPI) [9,10]. Although its use as a backward mode photoacoustic sensor has been proposed[11], its application to date has been limited to forward mode photoacoustic imaging[12] on account of the opaque aluminium coatings used to form the mirrors of the FPI. In this paper, we describe a new sensor design that employs wavelength selective dielectric mirror coatings in order to make the sensor transparent to excitation laser pulses at 1064nm, thereby enabling it to be used in backward mode.

In section 2.1 the Fabry Perot (FP) sensor design and fabrication is described. In section 2.2, the angle-tuned optical system used to interrogate the sensor and map its output is described. In section 3, images of phantoms comprising planar and cylindrical absorbers immersed in a scattering liquid are presented and used to demonstrate the system and assess penetration depth and spatial resolution.

2. FP BACKWARD-MODE PHOTOACOUSTIC IMAGING SYSTEM

The photoacoustic imaging system comprises a FP polymer film sensor head that is placed in acoustic contact with the tissue surface. The mirrors of the FP sensor are designed to be highly reflective at 850nm but transparent at 1064nm enabling excitation laser pulses at the latter wavelength to be transmitted through the sensor into the underlying tissue. The resulting photoacoustic signals arrive at the sensor where they modulate the optical thickness of the polymer film, and therefore the reflectivity of the sensor at 850nm. By illuminating the sensor with a large diameter CW interrogating laser beam at this wavelength and mechanically scanning a photodiode over the reflected beam, the lateral and temporal distribution of the acoustic waves arriving at the sensor head can be mapped. In this way the system can be regarded as a notional ultrasound array, the aperture of which is defined by the dimensions of the scan region and the element size and interelement spacing by the sensitive area of the photodiode and the scan increment respectively.

2.1 FP sensor design and fabrication

A schematic and photograph of the FP sensor head is shown in figure 1. It comprises a 4mm thick wedged glass backing stub on to which a 19 layer SiO_2/TiO_2 dielectric stack was vacuum deposited to form the first FPI mirror. This was followed by the vacuum deposition of a 60μm thick Parlyene C polymer film spacer. A second SiO_2/TiO_2 dielectric stack was deposited on to the Parylene layer to form the second FPI mirror. Finally, the entire structure was encapsulated within a 2μm thick Parylene C to prevent water ingress damaging the external dielectric mirror. The dielectric mirrors of the FP cavity were of a long pass optical filter design with high transmission (>99%) at the photoacoustic excitation wavelength of 1064nm and high (>89%) reflectivity at the sensor interrogation wavelength of 850nm.

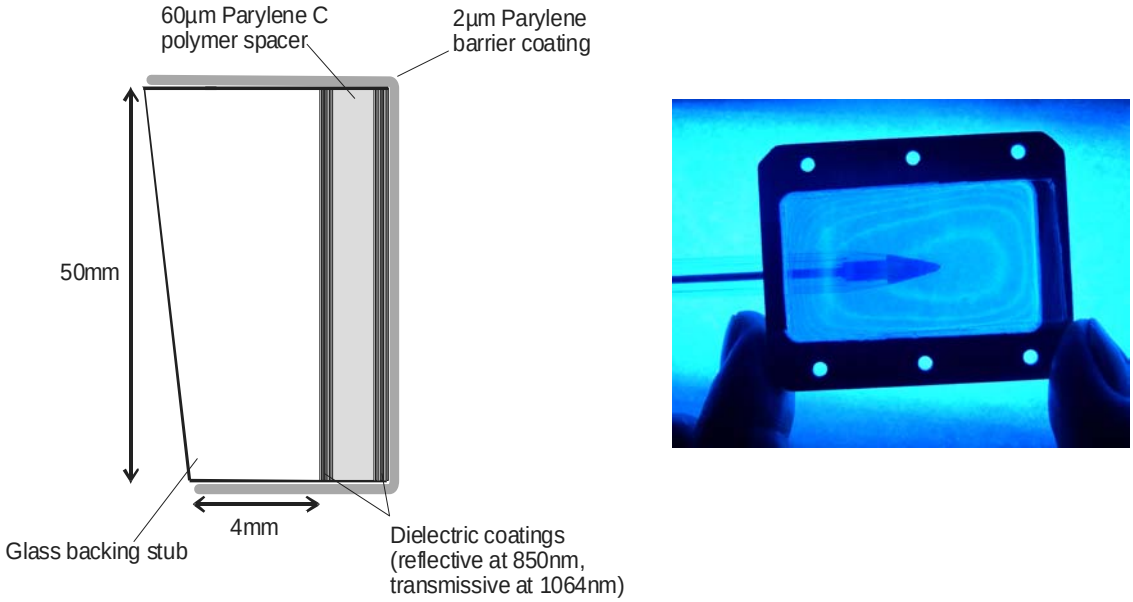

Figure 1 Schematic and photograph of backward-mode FP sensor head. The photograph shows the sensor (wedge side uppermost) under narrow band UV illumination illustrating the concentric elliptical FPI transmission fringes and the transparent nature of the sensor head.

2.2 Optical interrogation and mapping system

Figure 2 shows a schematic of the experimental system used to map photoacoustic signals in backward mode. The output of a CW 850nm DBR laser diode is collimated and expanded to a diameter of 12mm and used to illuminate the sensor via a PC controlled precision galvanometer and a 1-1 beam expander comprising lenses L1 and L2. The reflected output of the sensor is directed via a beamsplitter and lens L3 on to a 25MHz silicon pin photodiode of aperture 0.4mm mounted on an precision x-y scanning stage under PC control. Excitation pulses of 7ns duration provided by a Q-switched Nd:YAG laser operating at 1064nm are delivered though the sensor and into the target via a 1mm diameter multimode optical fibre. The excitation beam diameter at the surface of the sensor was approximately 15mm.

In principle, the photoacoustic signals incident on the sensor could be mapped by scanning the photodiode over the reflected output beam at P2 and recording the detected acoustic waveform at each point. However, a difficulty arises in that the sensitivity of the sensor varies from point to point due to variations in the phase bias or working point of the interferometer due to changes in the optical thickness of the polymer film. To overcome this problem, the optical pathlength of the FPI and hence the phase bias, is optimally set for each point of the scan by adjusting the angle of the beam incident on the sensor[13,12]. This is achieved using the optical subsystem comprising the galvanometer mirror and lenses L1, L2 and L3 shown in figure 2. Since the galvanometer mirror and the FP sensor are situated in the back and front focal planes of L1 and L2 respectively, a change in the input angle θ_i produces a corresponding change in the angle θ_0 of the beam incident on the sensor at P1 without translation. The beam reflected from the sensor is equivalently reversed through the system via lens L3 on to the photodiode at P2. Since P2 lies in the focal plane of L3 there is also no translation of the beam incident on the photodiode as θ_i is varied. By ensuring that the optical beams pivot about P1 and P2 in this way, the 1-1 spatial correspondence between the acoustic detection point at the FP sensor head and its corresponding optical detection point at P2 is preserved. Using this system, the interference fringes of the FPI (seen in transmission in the photograph in figure 1), the spatial derivatives of which can be thought of as contours of constant sensitivity, can be scanned across the illuminated area of the sensor enabling any point to be interrogated with optimum sensitivity.

In practice, the optimum phase bias point is located by rotating the galvanometer mirror such that the beam incident on the sensor is swept from normal incidence through an angle of 10 degrees. The output of the photodiode is monitored during this process to provide the angle tuned intensity-phase transfer function (ITF) of the interferometer. The derivative of the ITF (a measure of the interferometric phase sensitivity) is then calculated and the mirror returned to the angle corresponding to the peak value of the ITF derivative - the point of maximum sensitivity. When scanning the photodiode in order to map an incident acoustic field, this phase bias control procedure is repeated at each point of the scan prior to capturing the photoacoustic waveform. Since the ITF derivative provides a measure of the sensor sensitivity, it can be used to correct for any sensitivity variations due to changes in intensity across the illumination beam or imperfections in the sensing film. This was implemented by dividing the waveform captured at each point of the photodiode scan by the peak value of the ITF derivative obtained at that point.

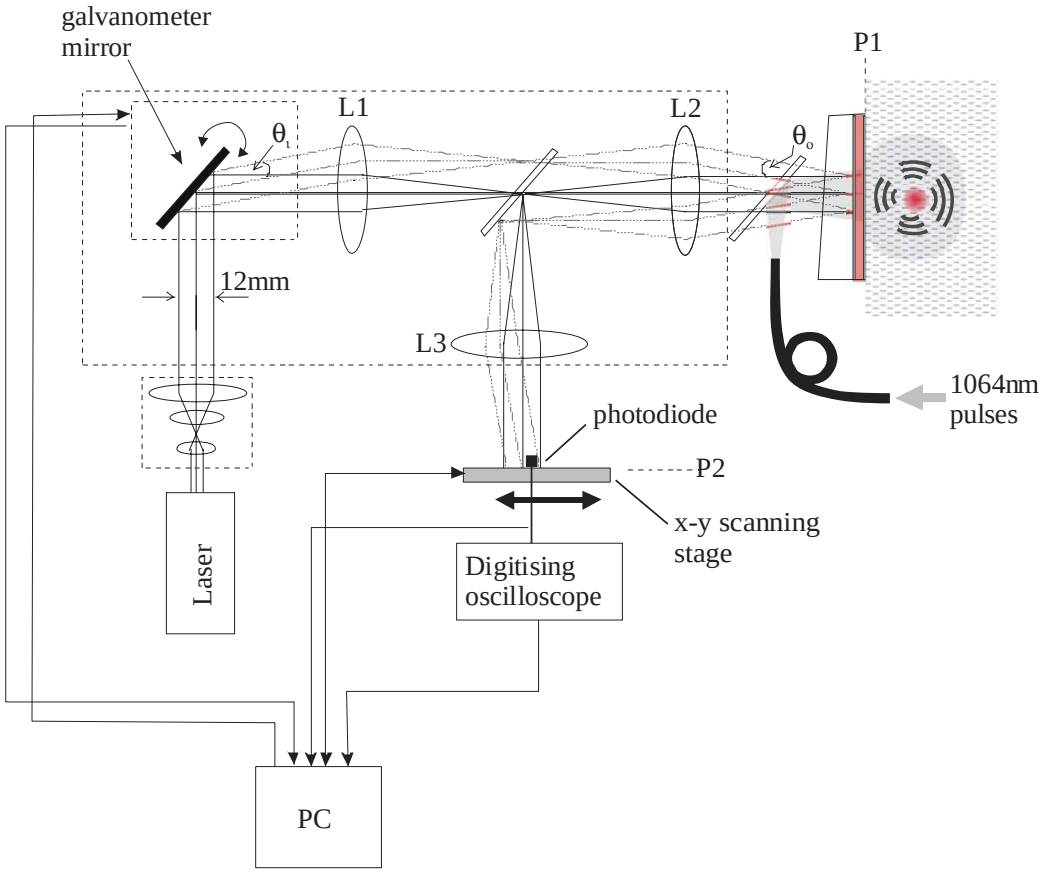

Figure 2 Backward-mode, angle-tuned photoacoustic imaging system

3. RESULTS

To evaluate the system, experiments in phantoms comprising various absorbing structures immersed in a scattering liquid were performed. In each case the background scattering liquid was a 10% aqueous solution of Intralipid-10% of reduced scattering coefficient $\mu_s'=1mm^{-1}$ and absorption coefficient $\mu_a=0.03mm^{-1}$ at 1064nm - the excitation wavelength used for these experiments. These optical properties are approximately representative of tissues such as the breast[14] and skin[15]. The beam diameter and pulse energy of the 1064nm excitation laser pulse were such that the incident surface fluence was always significantly less than $0.1J/cm^2$ - the maximum permitted exposure (MPE) level for nanosecond NIR pulsed laser irradiation

incident on skin[16].

3.1 Depth profiling of planar absorbers

A simple "line-of-sight" depth profiling experiment was performed to provide an indication of the lateral dimensions over which photoacoustic signals could be mapped (the "array" aperture), the depth at which signals generated in an absorber of physiologically realistic optical properties could be detected and to assess vertical spatial resolution. To achieve this, 2 plastic sheets, one of thickness 1.3mm and absorption coefficient μ_a=0.8mm^{-1} and the other 100µm thick and of μ_a=18mm^{-1} were positioned approximately 12mm from the sensor within an Intralipid solution as shown in figure 3. The absorption coefficient of the 1.3mm thick absorber was chosen to provide an absorption contrast comparable to that of fully oxygenated blood at 1.06µm[17]. The purpose of the more strongly absorbing 100µm target was to provide a means of estimating axial spatial resolution rather than be representative of any particular tissue-optical properties. The excitation laser beam was directed through the sensor into the Intralipid and the photoacoustic signals mapped by scanning the photodiode along a line of length 11mm in 0.2mm steps across the sensor output beam. At each point of the scan, the detected photoacoustic waveform was averaged over 200 laser shots and downloaded to a PC. Each detected waveform was linearly mapped to a grayscale and aligned vertically along the line-of-sight of the detector position at which it was captured to provide the image shown in figure 3 – a specific form of image reconstruction, valid only for the special circumstances of a planar, and therefore 1 dimensional, source geometry as in this experiment.

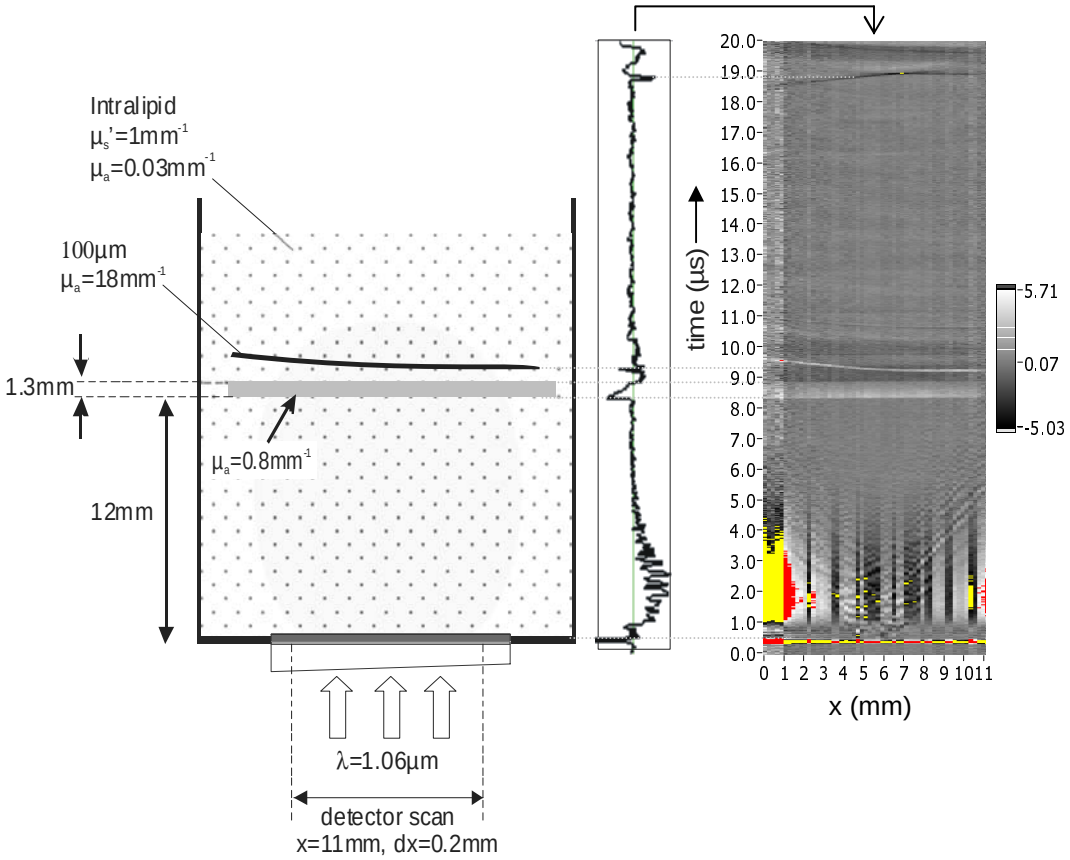

Figure 3 Backward-mode depth profile of planar absorbers immersed in Intralipid. The waveform in the centre shows the signal recorded at the centre of the scan. The image on the right is a linear grayscale mapping of the photoacoustic signals captured over the 11mm linescan. Photodiode aperture: 0.4mm, incident laser fluence: 0.05 J/cm^2

The 2 absorbers are clearly identifiable in figure 3 and their thickness and vertical position, calculated using the speed of sound in the polymer and water respectively, are in agreement with the known values. The vertical spatial resolution, limited by the acoustic thickness of FP polymer sensing film, is approximately 100μm.

Two forms of artefact are evident in the image in figure 3. The alternating light and dark vertical bands, which are visible for t<~5μs, represent the slow recovery of the photodiode following its saturation by the high intensity 1064nm excitation pulses at t=0. The polarity of these vertical line features appears to switch randomly from point to point along the linescan. This is because, at each point of the scan, the phase bias control system can select either a peak positive or a peak negative ITF derivative to settle on – the choice is arbitrary as both are optimal due to the symmetrical nature of the ITF. If the ITF derivative is negative, the system software inverts the captured time record to ensure the photoacoustic waveform retains the correct polarity. However, in doing so, non acoustic features which are independent of the ITF slope, such as those corresponding to the photodiode saturation, also become inverted. The variation in the sign of the vertical line artefacts can therefore readily be avoided by forcing the system to settle on a positive ITF slope only. This was implemented for the experiment carried out in the following section. The second type of artefact evident in figure 3 comprises the V-shaped wavefronts that appear to originate from point sources close to the sensor. These are thought to be due to aggregation of the particulate components of Intralipid on the detector surface producing regions of increased scattering and possibly absorption which act as localised sources of spherical waves.

3.2 2D imaging of line sources

To test the ability of the system to image discrete absorbers, a 3-layer structure consisting of strongly absorbing parallel lines of width 0.076mm and 0.86mm separation that were laser printed on to transparent acetate sheets was used. This was immersed in the Intralipid solution and placed parallel to, and 6.2mm above, the sensor as shown in figure 4. When irradiated with pulsed laser light, the target approximates to a series of parallel line sources. The photodiode was scanned along a 10mm line in steps of 0.2mm. At each point of the scan, the detected photoacoustic waveforms were averaged over 50 laser pulses and downloaded to the PC.

Unlike the highly directional 1D planar sources used in the previous section, the line absorbers in figure 4 emit cylindrical wavefronts into 2π radians. It is therefore no longer appropriate to form an image by assuming that a signal arriving at the detector must have originated from a source lying directly along its vertical line of sight. The more general time domain radial backprojection or **k**-space approaches to photoacoustic image reconstruction, which reconstruct for an arbitrary 2D or 3D initial source/stress distribution, are required. In this case, the problem was regarded as one of 2D as the line sources on the acetate sheets were aligned orthogonal to the detector scan line and assumed to be of infinite extent in the y-direction. A 2D inverse **k**-space method[18] was used to reconstruct the initial stress distribution from the signals detected over the line scan. This approach is based upon the premise that the spatial frequency components of the initial stress distribution $P_o(x, y)$ are directly mapped on to, and can therefore be recovered from, the spatial and temporal frequency components of the set of detected pressure signals p(x, t). The derivation and computational implementation of this method are described in detail in references 18 and 19. Briefly however, it requires (1) taking a 2D Fourier transform of the detected pressure signals p(x, t) to obtain $A(k_x, \omega)$, where k_x is the horizontal spatial frequency, (2) transforming ω to the vertical spatial frequency k_z using the dispersion relationship ($\omega = c \cdot \sqrt{k_x^2 + k_z^2}$) to obtain $A(k_x, k_z)$, (3) rescaling $A(k_x, k_z)$ using an algebraic operator[18] to obtain the spatial frequency components of the initial stress distribution $P(k_x, k_z)$ and (4) inverse Fourier transforming $P(k_x, k_z)$ to obtain the required initial stress distribution $P_o(x, z)$. The advantage of this approach over back projection methods is that it provides, in principle, an exact reconstruction (assuming only propagating waves are detected) resulting in fewer artefacts. It is also significantly faster due the computational efficiencies gained through use of the FFT – the reconstruction time for the image shown in figure was approximately 1 second.

The reconstructed image in figure 4 shows the sources in the lower 2 layers of the target distributed at the correct height and separation. The lateral spatial resolution is, by analysis of the edges of one of the reconstructed sources located in the lower acetate sheet, conservatively estimated at 0.4mm, limited by the photodiode aperture. The thickness of the ink deposited on to the acetate sheet is not known accurately but is likely to be significantly less than 10μm, thus approximating to a spatial impulse function in the vertical direction. Thus by measuring the thickness of one of the

reconstructed sources the spatial resolution is estimated at 100µm, limited by the acoustic thickness of the Fabry Perot polymer sensing film.

The sources on the third (uppermost) layer are almost invisible in the reconstructed image. This was something of a surprise as when the same phantom was imaged under identical conditions in forward mode, all 3 layers were clearly visible on the reconstructed image. This is because the detected signal amplitude depends on the source strength, which decreases approximately exponentially with increasing distance from the illuminated surface due to optical absorption and scattering. It also falls off with increasing source-detector separation due to geometrical spreading of the acoustic wavefront. In backward mode, both effects combine to produce a rapid fall off in the detected signal amplitude with source depth. In forward mode however, the effect of optical attenuation is partly ameliorated by the reduction in the spreading of wavefront since the source-detector separation decreases with increasing source depth. Hence there is an apparent increase in the depth at which a target can be imaged in forward mode.

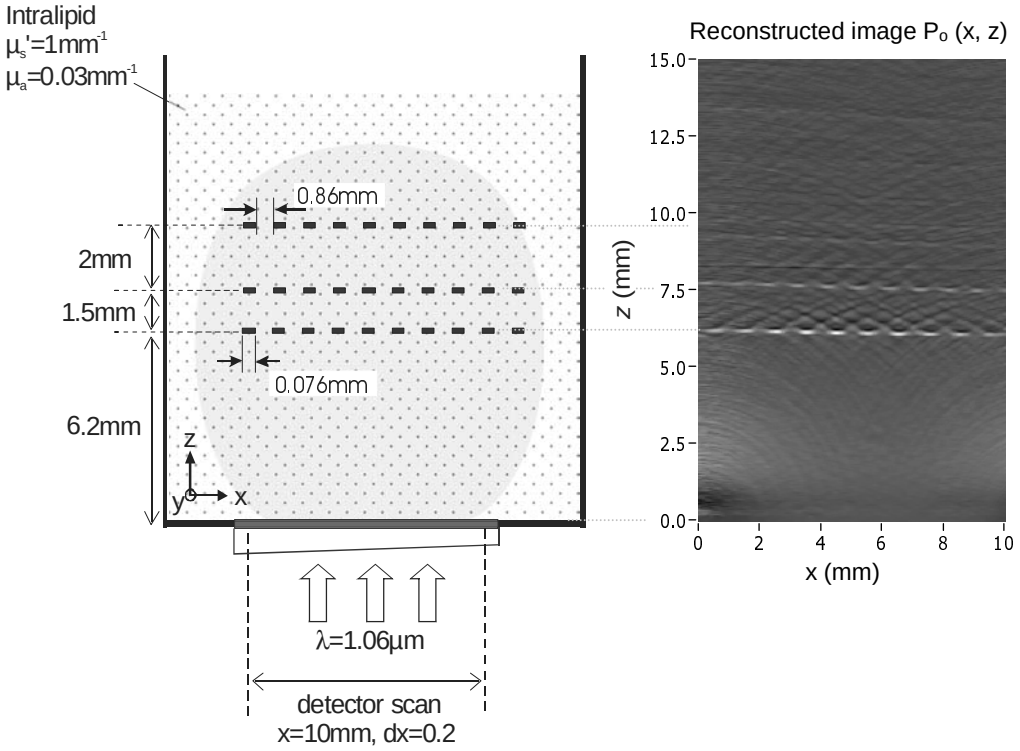

Figure 4 2D imaging of a 3-layer line source phantom. Photodiode aperture: 0.4mm, incident laser fluence: 0.015 J/cm^2

4. CONCLUSIONS

The feasibility of using the Fabry Perot polymer film sensing concept for backward photoacoustic imaging has been demonstrated. The depth profiling experiment described in section 3.1 confirms our previous work[12] that indicated the detection sensitivity (of almost overriding concern in biomedical photoacoustic imaging) of this type of sensor will be sufficient for visualising blood vessels within several mm of the skin surface. Two key improvements are required for *in vivo* use: the lateral spatial resolution needs to be increased and the acquisition time reduced. Future work is to focus on meeting these demands by addressing the FP sensor head with an optically scanned focussed spot. It should then be possible to provide sub-50µm element sizes and 1D or 2D array apertures of 2-3cm to improve lateral resolution and acquire photoacoustic waveforms at intervals of a few tens of milliseconds compared to the current 2-3 seconds.

ACKNOWLEDGEMENTS

This work is supported by the UK Engineering and Physical Sciences Research Council (EPSRC).

REFERENCES

[1] X. Wang, Y. Pang, G. Ku, X. Xie, G. Stoica, and L. V. Wang, "Noninvasive laser-induced photoacoustic tomography for structural and functional in vivo imaging of the brain," Nature Biotechnology **21**(7), pp. 803–806, 2003

[2] Oraevsky AA, Savateeva EV, Solomatin SV, Karabutov A, Andreev VG, Gatalica Z, Khamapirad T, and Henrichs PM, Optoacoustic imaging of blood for visualization and diagnostics of breast cancer, Proc. SPIE 4618, pp81-94, 2002

[3] Paltauf G., Koestli K, Frauchiger D, Frenz M., Spectral optoacoustic imaging using a scanning transducer, Proc. SPIE Vol. 4434, p. 81-88, 2001

[4] Viator JA, Au G, Paltauf G, Jacques SL, Prahl SA, Ren H, Chen Z, Nelson JS, Clinical testing of a photoacoustic probe for port wine stain depth determination, Lasers in Surgery and Medicine, **30**, pp141-148, 2002

[5] Pilatou MC, Kolkman RGM, Hondebrink E, Berendsen R, De Mul FF, Photoacoustic imaging of microvascular structure in tissue, Proc SPIE Vol 3916, pp 48-54, 2000

[6] Karabutov AA, Savateeva EV, Podymova NB, Oraevsky AA, Backward mode detection of laser induced wideband ultrasonic transients with optoacoustic transducer, Journal of Applied Physics, Vol 87, No 4, pp2003-2014m 2000

[7] B Payne BP, Venugopalan V, Mikic BB, Nishioka NS, Optoacoustic tomography using time resolved interferometric detection of surface displacement, Journal of Biomedical Optics, **8**(2), pp273-280, 2003

[8] Koestli K, Frenz M, Weber HP, Paltauf G, Schmidt-Kloiber H, Optoacoustic tomography: time-gated measurement of pressure distributions and image reconstruction, Applied Optics, Vol. 40, No 22, pp3800-3809, 2001

[9] *Beard PC, Perennes F, Mills TN, Transduction mechanisms of the Fabry Perot polymer film sensing concept for wideband ultrasound detection., *IEEE Transactions on Ultrasonics, Ferroelectrics and Frequency control*, Vol 46, No 6, pp1575-1582, 1999

[10] *Beard PC and Mills TN, A 2D optical ultrasound array using a polymer film sensing interferometer, 2000 IEEE Ultrasonics Symposium, pp1183-1186, 2000

[11] *Beard PC and Mills TN, An optical detection system for biomedical photoacoustic imaging, Proc. SPIE 3916, pp100-109, 2000

[12] *Beard PC , Photoacoustic imaging of blood vessel equivalent phantoms, Proc, SPIE, Vol 4618, p54-62, 2002

[13] *Beard PC, Interrogation of Fabry Perot sensing interferometers by angle tuning, *Measurement Science and Technology*,14, pp 1998 – 2005, 2003

[14] Troy TA, Page DL, Sevic-Mucraca EM, Optical properties of normal and diseased breast tissues: prognosis for optical mammography, J Biomed Optics, 1(3), pp342-355, 1996

[15] Simpson, C.R., Kohl, M., Essenpreis, M., Cope, M., "Near-infrared optical properties of ex vivo human skin and subcutaneous tissues measured using the Monte Carlo inversion technique," Phys. Med. Biol. 43, 2465-2478 (1998).

[16] British Standard, BS EN60825-1, 1994

[17] Roggan A, Friebel M, Dorschel K, Hahn A, Muller G, Optical properties of circulating human blood in the wavelength range 400-2500nm, Journal of Biomedical Optics, 4(1), pp36-46, 1999

[18] *Köstli KP and Beard PC, Two-Dimensional Photoacoustic Imaging by Use of Fourier-Transform Image Reconstruction and a Detector with an Anisotropic Response, *Applied Optics*, Volume 42, Issue 10, 1899-1908, 2003

[19] Köstli K, Frenz M, Bebie H, Weber H, Temporal backward projection of optoacoustic pressure transients using Fourier transform methods, Physics in Medicine and Biology, **46,** pp1863-1872, 2001

* *Downloadable at: http://www.medphys.ucl.ac.uk/research/borl/pub_alph.htm*